GSA Data Repository 2017164

Edward W. Marshall, John C. Lassiter, Jaime D. Barnes, Ambre Luguet, and Moritz Lissner, 2017, Mantle melt production during the 1.4 Ga Laurentian magmatic event: Isotopic constraints from Colorado Plateau mantle xenoliths: Geology, doi:10.1130/G38891.1

Appendix 1

Sample Petrology:

This section presents a mineralogic and petrographic summary of each sample. Mineral modal abundances are visually estimated in thin section, not point counted. All samples were spinel peridotites, except N23-GN, EMGN21, EMGN24, N106-GN and N55-GN. N23-GN was interpreted by Roden et al. (1990) to have been garnet peridotite with garnets having been replaced by chlorite. Their interpretation was based largely on HREE depletion in clinopyroxene, which is typical of cpx in equilibrium with garnet, and the garnet-like shape of the chlorite clusters. We have identified two other xenoliths with cpx REE patterns similar to N23-GN: EMGN21 and EMGN24. Both of these samples have depleted HREE concentration and chlorite interpreted as replacing garnet, similar to N23-GN. N55-GN has garnet rims around Al-spinel cores (see Smith and Levy, 1976). N106-GN was noted to have garnet rims around spinel (personal communication, D. Smith), but we were unable to confirm this texture.

Our petrologic observations agree with the findings of Smith (1979) that Green Knobs (35.9533° N, 109.0227° W) xenoliths have three hydrous peridotite assemblages:

1) Mineral assemblages that contain *aluminous-spinel* (Al-Spinel) and are poor in hydrous phases (~ <5% by mode).

2) Mineral assemblages that contain amphibole and chlorite. These samples generally all contain *chlorite clusters*-- a textural feature formed by aluminous phases (e.g., Al-spinel, garnet) reacting with fluid and olivine to form chlorite. In spinel peridotites, these chlorite clusters contain Cr-spinel interpreted to be the Al-depleted reaction product of the original Al-spinel.

3) Mineral assemblages that contain *abundant antigorite* relative to the other two assemblage types (>5% by mode). A key textural feature of this assemblage is that platy antigorite crystals are found throughout the sample. In addition, antigorite rims chlorite clusters and individual chlorite grains. This assemblage typically contains chlorite and amphibole in addition to serpentine.

Moses Rock (37.1081°N, 109.7841°W) peridotite xenoliths contain similar textures to Green Knobs peridotites and range from nearly anhydrous peridotites to fully hydrated assemblages (assemblages containing only hydrous phases with rare/absent relict grains, e.g. EMMR4). On average, Moses Rock xenoliths tend to have a greater abundance of hydrous minerals compared to Green Knobs, as McGetchin and Silver (1970, 1972) found spinel peridotite much less abundant than "serpentine schist."

Moses Rock

MR-ATG-13 (Sample collected by Anna T. Gavasci)

Mineralogy: ol + opx + cpx + serpentine + Al-spinel

Petrography: Spinel lherzolite with large (>5mm) opx porphyroblasts. Olivine is fractured with serpentine commonly filling the fractures. Opx, cpx, and spinel are not fractured. Serpentine < 10% by mode.

Location: 37.1081°N, 109.7841°W

EMMR4:

Mineralogy: Serpentine + amphibole + chlorite + opaque

Petrography: Serpentinite. All primary silicate minerals have been reacted to serpentine, chlorite and/or amphibole; no relict grains are observed in thin section. However, relict grains were found in crushed mineral separates. Thin bands of opaque minerals (likely Cr-spinel) appear to define the grain boundaries of the serpentine and amphibole pseudomorphs. Chlorite clusters surround opaques. Fibrous amphibole grows irregularly in clusters, and along cleavages in pseudomorphous serpentine. Serpentine ~80% by mode, amphibole ~10%, chlorite ~5%,

Location: 37.1081°N, 109.7841°W

EMMR25

Mineralogy: Ol + opx + chlorite + cpx + amphibole + serpentine + opaque

Petrography: Hydrated lherzolite. ~1 cm clusters of chlorite surround opaques, most likely Cr-spinel. Prismatic amphibole grows along the grain boundaries of pyroxenes and rim chlorite clusters. Chlorite forms centimeter-scale clusters around spinel, but also is found intergrown with clinopyroxene. Olivine is fractured throughout the thin section, and these fractures are filled with serpentine.

Location: 37.1081°N, 109.7841°W

Green Knobs

EMGN2

Mineralogy: Ol + opx + cpx + Al-Spinel + serpentine

Petrography: Deformed equigranular spinel lherzolite. Grain boundaries are filled with very tiny, high birefringence grains. These small grains have optical properties consistent with olivine and pyroxene, but are too small to confirm. Olivines have undulose extinction and pyroxenes are kinked. Olivine is fractured, with fractures containing serpentine. Cpx is cloudy with inclusions too small to identify. Spinel is not opaque. Serpentine growth is limited to fractures and grain boundaries, making up less than 5% by mode.

Location: 35.9533° N, 109.0227° W

EMGN6

Mineralogy: Ol + opx + serpentine + amphibole + chlorite + cpx

Petrography: Hydrated equigranular peridotite. Amphibole forms twinned, prismatic prisms that incompletely replace pyroxenes. Amphibole tends to grow across grain boundaries as far as the cores of some grains, rather than forming rims. Amphibole commonly contains abundant opaque inclusions. Chlorite is limited to thin rims around opaque grains. Occasionally chlorite is found as inclusions within amphiboles. Serpentine occurs throughout the section as slender prismatic crystals, rimming chlorite, and included in amphibole, pyroxenes and olivine. Serpentine is sometimes intergrown with amphibole and chlorite. Olivine is replaced by serpentine heterogeneously-- some olivine grains have a small amount of serpentine in fractures, other grains are almost entirely replaced as serpentine replaces olivine along [010] cleavages. A vein, now filled with serpentine, cuts across the thin section. Serpentine 15% by mode, amphibole 15% by mode, chlorite 5% by mode.

Location: 35.9533° N, 109.0227° W

EMGN9

Mineralogy: Ol + opx + chlorite + opaque + amphibole + serpentine

Petrography: Deformed, hydrated equigranular peridotite, containing very large (>8mm) chlorite clusters around opaques. Cpx was not found in thin section, and has most likely been reacted to amphibole. Cpx was found in mineral separates. Olivine [010] cleavages define a foliation in the peridotite. Amphibole grows in prismatic grains that replace pyroxenes. Serpentine grows across pyroxenes with fanning bunches of crystals. Serpentine forms irregular masses within olivines. Chlorite is ~20-25%, amphibole ~5%, serpentine is <5% by mode.

Location: 35.9533° N, 109.0227° W

EMGN12

Mineralogy: Ol + Opx + amphibole + chlorite + serpentine + opaque

Petrography: Hydrated equigranular peridotite. Olivines and opx form a mosaic texture, typical of mantle peridotites. Olivine is fractured and contains serpentine in the fractures. Amphibole replaces pyroxene. Chlorite forms clusters around opaques and is also found intergrown with amphibole. Chlorite ~10%, amphibole ~10%. serpentine ~ 1% by mode.

Location: 35.9533° N, 109.0227° W

EMGN21

Mineralogy: Ol + opx + chlorite + serpentine + opaque.

Petrography: Hydrated equigranular harzburgite.

Depleted HREE in EMGN21 cpx supports the idea that EMGN21 was a garnet peridotite before all garnet in the sample was reacted to chlorite.

Olivine displays [010] cleavage. The olivine cleavage fractures are filled with serpentine. Chlorite forms clusters, containing few opaques. Olivine and opx are commonly cut across by serpentine. Cpx was not found in thin section, but was found in mineral separates. Chlorite ~10% by mode, serpentine ~7% by mode.

Location: 35.9533° N, 109.0227° W

EMGN24

Mineralogy: Ol + opx + serpentine + amphibole + chlorite + opaques + clinohumite + carbonate

Petrography: Hydrated equigranular peridotite. Depleted HREE in EMGN24 cpx indicate that EMGN24 was garnet bearing prior to hydration. Chlorite clusters surround aggregates of small opaque grains. Chlorite clusters are small (~1400 μm), but are abundant in contrast to samples that have fewer, larger chlorite clusters (e.g., EMGN9). Chlorite and amphibole frequently grow within and surround opx. Cpx was not observed in thin section, but found in mineral separates. Dense intergrowth clusters of chlorite and amphibole may be a hydration product of Al-rich cpx. Serpentine rims chlorite clusters and forms slender crystals growing within and around pyroxenes and olivines. Carbonate is present as a long vein that cuts across the thin section.

Serpentine is ~15%, chlorite is ~10%, amphibole ~5%, clinohumite is <1% by mode.

Location: 35.9533° N, 109.0227° W

EMGN27

Mineralogy: Ol + opx + serpentine + amphibole + carbonate + chlorite + cpx + opaques

Petrography: Hydrated equigranular harzburgite. Olivine displays [010] cleavage, made visible by thin fractures filled with serpentine. Serpentine also forms irregular-shaped clumps that grow within olivines. Chlorite thinly rims opaques (tens of microns thick). Prismatic amphibole can rarely be found replacing pyroxenes. Three carbonate grains in this section contain inclusions of silicate minerals, likely opx. Serpentine ~ 15% by mode, chlorite ~ 1%, amphibole ~1% by mode.

Location: 35.9533° N, 109.0227° W

EMGN29

Mineralogy: Ol + opx + cpx + chlorite + amphibole + opaque + serpentine

Petrography: Lherzolite, modal olivine abundance (~50%) is similar to modal pyroxene abundance (~50%). EMGN29 has very little textural overprinting by hydrous mineral growth. Olivines have curved boundaries with pyroxenes, but with other olivines they have straight boundaries with 120° triple junctions. Olivines and pyroxenes may display undulose extinction. Finer sized cpx, amphibole and chlorite (~ 50 μm) are found at some junctions and grain boundaries. Cpx has two populations, larger (~1500 μm) grains similar in size to olivine and opx in the section, and small (~500 μm) grains that are found in the interstities of larger grains. Cpx (of both sizes) is frequently cloudy with inclusions. Chlorite surrounds opaque grains. Serpentine fills fractures in olivine. Serpentine, amphibole and chlorite make up ~ 1% of the sample by mode.

Location: 35.9533° N, 109.0227° W

EMGN37

No thin section.

Location: 35.9533° N, 109.0227° W

N16-GN

Mineralogy: Ol + Al-spinel + cpx + opx + serpentine

Petrology: Equigranular spinel lherzolite. Olivines and pyroxenes show minor undulose extinction. Sample is close to textural equilibrium, containing many 120° triple junctions. Hydrous minerals are limited to grain boundaries and fractures. Serpentine is ~5% by mode.

Previous studies also using this sample: Smith and Levy, 1976; Roden et al., 1990; Roden and Shimizu, 1993; Smith, 2013; Behr and Smith, 2016**.**

Location: 35.9533° N, 109.0227° W

N17-GN

Mineralogy: Ol + opx + cpx + chlorite + serpentine + amphibole + opaque

Petrology: Equigranular lherzolite-harzburgite. Thin chlorite rims surround opaques. Larger Al-spinel grains have opaque rims with semi-transparent cores. Serpentine fills fractures and grain boundaries. Amphibole grows in grain boundaries around pyroxenes. Olivines and pyroxenes display kinking and undulose extinction. Chlorite ~1%, Amphibole <1%, serpentine <1% by mode.

Previous studies also using this sample: Smith and Levy, 1976; Smith, 1979; Roden and Shimizu, 1993; Smith, 2013.

Location: 35.9533° N, 109.0227° W

N23-GN

Mineralogy: Ol + opx + chlorite + cpx + amphibole + clinohumite + opaque

Petrography: Hydrated lherzolite. Chlorite forms round clusters that are rimmed with amphibole, but contain no opaques. The clusters make up ~10% of the sample. Roden et al. (1990) interpreted N23-GN to be a garnet peridotite prior to hydration, based on HREE depletions in cpx and the similarity of the shape of the chlorite clusters to garnets. Cpx is noticeably exsolved and is often rimmed with fine grained amphibole and chlorite. Chlorite ~ 25%, amphibole ~ 10% by mode.

Previous studies also using this sample: Smith, 1979; Roden et al., 1990; Roden and Shimizu, 1993; Smith, 2013.

Location: 35.9533° N, 109.0227° W

N53-GN

Mineralogy: Ol + opx + cpx + Al-spinel + serp

Petrology: Equigranular spinel lherzolite. Sample is close to textural equilibrium, containing many 120° triple junctions. In parts of the thin section, linear fractures containing fine grained, unidentified material cut across the sample. Serpentine fills thin cracks and grain boundaries, making up <1% by mode.

Previous studies also using this sample: Smith and Levy, 1976; Roden and Shimizu, 1993; Smith, 2013.

Location: 35.9533° N, 109.0227° W

N55-GN

Mineralogy: Ol + opx + cpx + sp + amph + serpentine + gar + serp

Petrology: Spinel-garnet lherzolite. Garnet rims spinel in irregularly thick rims. In places, clusters of neoblastic olivine, amphibole and chlorite occur at grain junctions. Amphibole grows around cpx, forming thin or partial rims of nucleating amphibole grains. Amphibole ∼1% by mode.

Previous studies also using this sample: Smith and Levy, 1976; Smith, 1979.

Location: 35.9533° N, 109.0227° W

N61-GN

Mineralogy: Ol + opx + cpx + Al-spinel +amph

Petrology: Equigranular spinel lherzolite. Similar to N53-GN, fractures cut across the sample containing unidentified, fine grained material. Unlike N53-GN, fine grained material can also be found at grain boundaries throughout the sample. Amphibole appears in a small cluster. Amphibole <1% by mode.

Previous studies also using this sample: Smith and Levy, 1976; Roden et al., 1990; Roden and Shimizu, 1993.

Location: 35.9533° N, 109.0227° W

N106-GN

Mineralogy: Ol + opx + cpx + chlorite + amphibole + opaques

Petrology: Hydrated lherzolite. Chlorite surrounds opaque grains. Fine grained amphibole surrounds cpx grains. Cpx is cloudy with inclusions. Cpx and opx are both intergrown with amphibole in places. One olivine porphyroblast is unusually long, almost 1cm in length. Garnet rims around spinel were reported in an informal description, but could not be confirmed (personal communication, D. Smith). Chlorite ~1%, amphibole ~10% by mode.

Location: 35.9533° N, 109.0227° W

N126-GN

Mineralogy: Ol + opx + cpx + Al-spinel + serpentine

Petrology: Spinel lherzolite. Sample is close to textural equilibrium, containing many 120° triple junctions. Olivines display undulose extinction. Evidence of hydration is limited to serpentine that fills thin fractures and grain boundaries. Serpentine <1% by mode. The rock has distinctive intergrowths of spinel and pyroxene, interpreted by Smith (1977) as products of garnet-olivine reaction.

Previous studies also using this sample: Smith, 1977.

Location: 35.9533° N, 109.0227° W

N178-GN

Mineralogy: Ol + opx + cpx + chlorite + Cr-spinel + phlogopite (trace)

Petrology: Deformed harzburgite. N178-GN is strongly foliated. Kinking of opx and olivine is found in almost all grains. Spinel is absent. Chlorite is present, but does not form clusters. Chlorite ~5% by mode.

Previous studies also using this sample: Smith, 2010; Smith, 2013.

Location: 35.9533° N, 109.0227° W

References

Behr, W.M., and Smith, D., 2016, Geochemistry, Geophysics, Geosystems: Geochemistry Geophysics Geosystems, v. 17, p. 2825–2834.

McGetchin, T.R., and Silver, L.T., 1972, A crustal-upper-mantle model for the Colorado Plateau based on observations of crystalline rock fragments in the Moses Rock Dike: Journal of Geophysical Research, v. 77, no. 35, p. 7022–7037.

McGetchin, T.R., and Silver, L.T., 1970, Compositional relations in minerals from kimberlite and related rocks in the Moses Rock dike, San Juan County, Utah: American Mineralogist, v. 55, no. 1618, p. 1738–1771.

Roden, M., and Shimizu, N., 1993, Ion microprobe analyses bearing on the composition of the upper mantle beneath the Basin and Range and Colorado Plateau provinces: Journal of Geological Research, v. 98, no. 93, p. 14091–14108.

Roden, M., Smith, D., and Murthy, V., 1990, Chemical constraints on lithosphere composition and evolution beneath the Colorado Plateau: Journal of Geophysical Research, v. 95, no. 89, p. 2811–2831.

Smith, D., 2010, Antigorite Peridotite, Metaserpentinite, and other Inclusions within Diatremes on the Colorado Plateau, SW USA: Implications for the Mantle Wedge during Low-angle Subduction: Journal of Petrology, v. 51, no. 6, p. 1355–1379.

Smith, D., 1979, Hydrous minerals and carbonates in peridotite inclusions from the green knobs and bull park kimberlitic diatremes on the Colorado Plateau: The Mantle Sample: Inclusion in Kimberlites and Other Volcanics, v. 16, p. 345–356.

Smith, D., 2013, Olivine thermometry and source constraints for mantle fragments in the Navajo Volcanic Field, Colorado Plateau, southwest United States: Implications for the mantle wedge: Geochemistry, Geophysics, Geosystems, v. 14, no. 3, p. 693–711.

Smith, D., 1977, The Origin and Interpretation of Spinel-Pyroxene Clusters in Peridotite: v. 85, no. 4, p. 476–482.

Smith, D., and Levy, S., 1976, Petrology of the Green Knobs diatreme and implications for the upper mantle below the Colorado Plateau: Earth and Planetary Science Letters, v. 29, p. 107–125.

Appendix 2

Samples and Analytical Methods

Sample Selection:

Peridotite xenoliths were collected from Green Knobs and Moses Rock in 2014. The collected peridotite xenoliths varied in size, texture, mineralogy and hydrous mineral abundance. We selected ~45 xenoliths that spanned this observed variability for further analysis. Additional samples that had been previously characterized were selected from the collection of Dr. Douglas Smith at The University of Texas at Austin. A small portion of each xenolith was crushed and 2-3 clinopyroxenes from each sample were mounted and analyzed by Electron Probe MicroAnalyzer (EPMA) to survey mineral major element variations. Based on these preliminary analyses, a suite of ~25 xenoliths were chosen for further study that span the observed range of compositions and textures.

Whole Rock Major and Trace Element Analyses

Analysis of major and trace elements in whole rock powders were performed at Washington State University GeoAnalytical Labs following the procedures of Johnson et al. (1999). For each sample, 5 to 10 grams of rock was powdered in a tungsten carbide (WC) swingmill at WSU. Whole rock major elements were determined via X-Ray Fluorescence (XRF), and trace element concentrations were determined via solution ICP-MS. Two powder duplicates, two grinding media duplicates, and BHVO-2 were all analyzed to test reproducibility and constrain potential contamination of the grinding media.

Tungsten carbide (WC) is commonly used for grinding samples in preparation for geochemical analysis because WC does not contaminate major elements. However, Hickson and Juras (1986) have suggested that WC may contaminate high field strength elements (HFSE, e.g., Ta, Nb). To test for possible HFSE contamination, separate splits from two samples (EMGN2 and EMGN23) were ground in WC and in agate for comparison. Ta concentrations were higher in the WC-ground powders for both samples, but were close to the detection limit. We did not observe a systematic increase in Nb in the WC-prepared powders or any other systematic differences for elements above detection limits.

Replicates of XRF powder splits are reproducible to better than 1% for elements with abundances greater than 5 wt% (Si, Fe, Mg), varied less than 5% for elements with concentrations between than 0.1 wt% and 5 wt% (Al, Cr, Mn, Ca, Na, Ni), and varied less than 10% for Ti (usually <0.1 wt%). Duplicate ICP-MS analyses varied within 5% for elements with abundances higher than 1ppm, and varied within 25% for concentrations less than 1 ppm. Analyzed replicates of BHVO-2 (See Table DR2) were within the published 2σ compositional variation of the standard.

Clinopyroxene Major Element Analyses

Clinopyroxene major elements were analyzed on a JEOL JXA-8200 EPMA at the University of Texas at Austin. EPMA analyses used a 20 nA beam current, 15 kV accelerating voltage, and a 10 μm defocussed beam. Count times were 30-40 s on peak and 15-20 s off peak, with shorter count times for more abundant elements. Precision of repeated analysis on secondary standard NMNH Cr-Augite 164905 (see Table DR1) for a given element is inversely correlated with that element's concentration. Reproducibility for elements with concentrations greater than 1 wt. % was better than 5%, and better than 12% for elements with concentrations less than 1 wt. %. Averaged analyses of NMNH Cr Augite were within 5% of the standard composition, except for Mn (within 12%) (Jarosewich et al., 1980). However because Al was calibrated using the Cr-Augite standard, NMNH Kakanui Hornblende 143965 was used as a secondary standard for this element. Reproducibility for Al on the Kakanui Hornblende standard was better than 2%. Probe analyses of the same cpx grain show similar reproducibility to the Cr-Augite standard for all elements except Ti, which has significantly worse reproducibility (141%) due to extremely low Ti concentration (<1000ppm) in most samples. Because Ti concentration by LA-ICP-MS has better reproducibility than the EPMA (1.5% on glass standards, 8% on grain duplicates) and because there is a 1:1 correlation between the EPMA and LA-ICP-MS datasets, we use Ti concentration data measured in clinopyroxene by LA-ICP-MS in place of data measured by EPMA. Clinopyroxenes in samples with chlorite growth typically display Al_2O_3 depletion in the edges of grains. Data presented in Table DR1 are average analyses of 4-5 cpx grain interiors from each sample. Previously published EPMA clinopyroxene analyses for two of the samples are available in Table DR1 for comparison with our results.

Clinopyroxene Trace Element Analyses

Clinopyroxene trace elements concentrations were measured via LA-ICP-MS using a New Wave UP-193FX laser system coupled to an Agilent 7500Ce quadrupole instrument at the University of Texas at Austin. The maximum spot size of 150 μm was used to achieve maximum signal intensity due to the low concentrations present for many trace elements. All spots were pre-ablated before analysis. Each individual laser ablation analysis consisted of a 40 sec gas blank followed by 60 sec laser dwell time. The laser wavelength was 193nm and had a 10 Hz firing rate. Ablated material was transported with a He sweep gas flow rate of 700 mL per min and Ar carrier gas flow rate of 650 mL per min. NIST 612 was used as the primary standard. Repeat analyses of the BCR-2G secondary standard are reproducible within 5% of the published composition, except for Pb, Hf, Gd, and Y which were reproduced within 8% of the published composition. Interior-to-edge variability is found in most Group T clinopyroxenes and in some Group D clinopyroxenes. In these samples, Sr and LREE concentration increases towards the edge of the grain. Typically, interiors of 4-5 clinopyroxene grains were analyzed per sample, using the same spots analyzed previously by EPMA. Data reported in Table DR1 are the average composition of these multiple grain interior analyses. In samples that do not contain interior-to-edge variation, clinopyroxene trace element concentrations from multiple grains are usually within 10%. In samples that do contain interior-to-edge variation, cpx trace element concentrations between multiple grains vary within the range of measured interior-to-edge variability.

Sm-Nd Isotope Analyses

Sm-Nd isotopes were measured on ~50 to ~200 mg of hand-picked cpx separates. Before digestion, the separates were either leached for 20 min in 2.5 N HCl at 60°C (soft leach) or for 1 hour in 6 N HCl at 90°C (hard leach). Samples were spiked with a ^{149}Sm-^{150}Nd mixed spike. The dissolution and chemical extraction procedures followed the procedures of Connelly et al. (2006). Following sample dissolution in $HF:HNO_3$, Nd and Sm were extracted via column chemistry using AG50W-X8 and HDEHP resins. Sm and Nd were loaded onto double Re filaments, and analyzed as metal ions on a Triton TIMS at the University of Texas at Austin. The full Nd procedural blank was less than 30 pg, and the full Sm procedural blank was less than 2.5 pg. The average $^{143}Nd/^{144}Nd$ value obtained at UT Austin for the AMES Nd standard during the period of this study was 0.512088±0.000013 (2σ), slightly higher than the value of Scher and Delaney (2010), 0.512069 ±0.000014. Similarly, the average composition of rock standard USGS BCR-2 measured during the same period was 0.512656±0.000014(2σ), slightly higher than the published composition of 0.512633 ±0.000007 (2σ) (Raczek et al., 2001). In order to eliminate inter-laboratory bias, the data have been adjusted by 0.000002, correcting to the published compositions of AMES and BCR-2 standards.

Clinopyroxene grains from hydrated xenolith assemblages usually contain fractures filled with hydrous minerals (e.g., chlorite, serpentine, amphibole) and often contain~~s~~ oxide and silicate inclusions. Most clinopyroxenes have a cloudy appearance and are not optically clear. As a result, completely optically pure separates could not be obtained. In addition, Group T cpx display LREE enriched rims, as observed in LA-ICP-MS core-to-rim profiles. This zoning may have affected Nd isotopes and Sm/Nd ratios in the rims relative to the cores. To constrain the influence of hydrous phases and LREE enrichment in the rims we analyzed duplicate cpx splits from three samples using two different leaching procedures. Nd isotope analyses using the two different procedures were reproducible within error for two samples. Nd isotopes for a third sample were higher by 2.89 epsilon units in the hard leach, but this split also had higher measured Sm/Nd, consistent with increased removal of the LREE-enriched rim component through the hard leach. Measured Sm/Nd compositions were variable in the different splits, but were not consistently higher in the hard leached splits relative to the soft leached splits. Variability in measured Sm/Nd and Nd isotope composition between different mineral splits from the same sample likely reflects in part differing abundances of inclusions in the separate splits. Despite this variability, isochron ages calculated from the Group D soft leach and hard leach samples yield similar ages (soft leach: 1.45 ±0.04 Ga, n=5; hard leach: 1.39 ±0.2 Ga, n=3). The Sm-Nd data are listed in Table DR4 for both soft and hard leach analyses. In Figure 3 and for calculation of the Group D isochron, we average the hard and soft leach data for each sample. The reported error is either the internal standard error of the measurement (2 SE) or two times the external standard error of the duplicates, whichever is greater.

Rhenium-Osmium Isotope Analyses

Re and Os were isolated from whole rock powders following the method of Byerly and Lassiter (2012). Most Re-Os digestions were performed at UT Austin. The Jackson School of Geosciences building at UT Austin was closed for renovations during the summer of 2015. A subset of samples was digested at the University of Bonn, Germany during the building closure. The digestion procedure at University of Bonn is similar to the procedure at UT Austin, except solvent extraction used chloroform instead of carbon tetrachloride. Rind-free chips of the xenoliths were cut with a water saw, and saw marks were removed with SiC sand paper. Chips were then ground to a fine powder in an alumina ball mill. Small amounts (~1.5-3 g) of powder were prepared in order to preserve as much of the xenoliths as possible for further analyses. As a result, intra-sample heterogeneity may not be fully homogenized by the small powder splits that were prepared. Separate chips were powdered for digestion at UT Austin and the University of Bonn. Approximately 1.5 g of whole rock powders were put in quartz pressure vessels, spiked with a ^{185}Re-^{190}Os mixed spike and then reacted in reverse aqua regia in a *Anton-Paar* High-Pressure Asher (at 105 bar and 300°C). Osmium was extracted from the aqua regia using CCl_4, and then back-extracted into HBr. The Os was purified further using microdistillation (Birck et al., 1997). Rhenium was separated from the aqua regia using anion exchange columns. Finally, Os was loaded onto Pt filaments, as described in Chatterjee and Lassiter (2015), and analyzed in negative ion mode (N-TIMS) as OsO_3^- on the Triton TIMS at UT Austin. Re was analyzed via solution MC-ICP-MS using the Micromass Isoprobe at UT-Austin, and on a Thermo Scientific Element XR SF-ICP-MS at University of Bonn. Total procedural Os blanks were <1pg at UT Austin and <2 pg at the University of Bonn. Re blanks were <5 pg. The average $^{187}Os/^{188}Os$ ratio of the Johnson-Matthey Os standard run during the period of this study was 0.113832 ±0.000006.

Osmium isotopes and Os concentration in replicate analyses (powders from separate xenolith chips) show greater variability than can be accounted for by analytical error. This may reflect variable sampling of different sulfide populations in the different xenolith splits and thus reflects intra-sample heterogeneity. From petrographic observation, many peridotite xenoliths from Green Knobs and Moses Rock contain abundant sulfides both as inclusions in silicate phases and along grain boundaries. In addition, EDS imaging of thin sections revealed the occasional presence of rare PGE alloy and PGE-sulfide grains, including a Ru-Rh-Ir alloy grain and PtS. Several analyses produced high Re concentrations (not quantitatively determined due to underspiking), which may have resulted from inclusion of Re-rich "nuggets". Despite the intra-sample heterogeneity, whole rock Al_2O_3 and $^{187}Os/^{188}Os$ are well correlated. For Figure 2, we report the average of replicate analyses. The reported error is either the internal standard error of the measurement (2 SE) or two times the external standard error of the replicates, whichever is greater. The data for all Re-Os replicate analyses can be found in Table DR3.

References

Birck, J.L., Barman, M.R., and Capmas, F., 1997, Re-Os Isotopic Measurements at the

Femtomole Level in Natural Samples: v. 20, p. 19–27.

Byerly, B.L., and Lassiter, J.C., 2012, Evidence from mantle xenoliths for lithosphere removal beneath the central Rio Grande Rift: Earth and Planetary Science Letters, v. 355–356, p. 82–93, doi: 10.1016/j.epsl.2012.08.034.

Chatterjee, R., and Lassiter, J.C., 2015, High precision Os isotopic measurement using N-TIMS: Quantification of various sources of error in 186Os/188Os measurements: Chemical Geology, v. 396, p. 112–123, doi: 10.1016/j.chemgeo.2014.12.014.

Connelly, J.N., Ulfbeck, D.G., Thrane, K., Bizzarro, M., and Housh, T., 2006, A method for purifying Lu and Hf for analyses by MC-ICP-MS using TODGA resin: Chemical Geology, v. 233, no. 1–2, p. 126–136, doi: 10.1016/j.chemgeo.2006.02.020.

Hickson, C.J., and Juras, S.J., 1986, Sample contamination by grinding.: Canadian Mineralogist, v. 24, no. 3, p. 585–589.

Johnson, D.M., Hooper, P.R., and Conrey, R.M., 1999, XRF Analysis of Rocks and Minerals for Major and Trace Elements on a Single Low Dilution Li-tetraborate Fused Bead: Advances in X-Ray Analysis, v. 41, p. 843–867.

Raczek, I., Jochum, K.P., and Hofmann, A.W., 2001, Neodymium and Strontium Isotope Data for USGS Reference GSP-1 , GSP-2 and Eight MPI-DING Reference Glasses: Geostandards Newsletterthe Journal of Geostandards and Geoanalysis, v. 27, no. 2, p. 173–179, doi: 10.1111/j.1751-908X.2003.tb00644.x.

Scher, H.D., and Delaney, M.L., 2010, Breaking the glass ceiling for high resolution Nd isotope records in early Cenozoic paleoceanography: Chemical Geology, v. 269, no. 3–4, p. 329–338, doi: 10.1016/j.chemgeo.2009.10.007.

Smith, D., 2010, Antigorite Peridotite, Metaserpentinite, and other Inclusions within Diatremes on the Colorado Plateau, SW USA: Implications for the Mantle Wedge during Low-angle Subduction: Journal of Petrology, v. 51, no. 6, p. 1355–1379, doi: 10.1093/petrology/egq022.

Appendix 3

Supplementary Figures

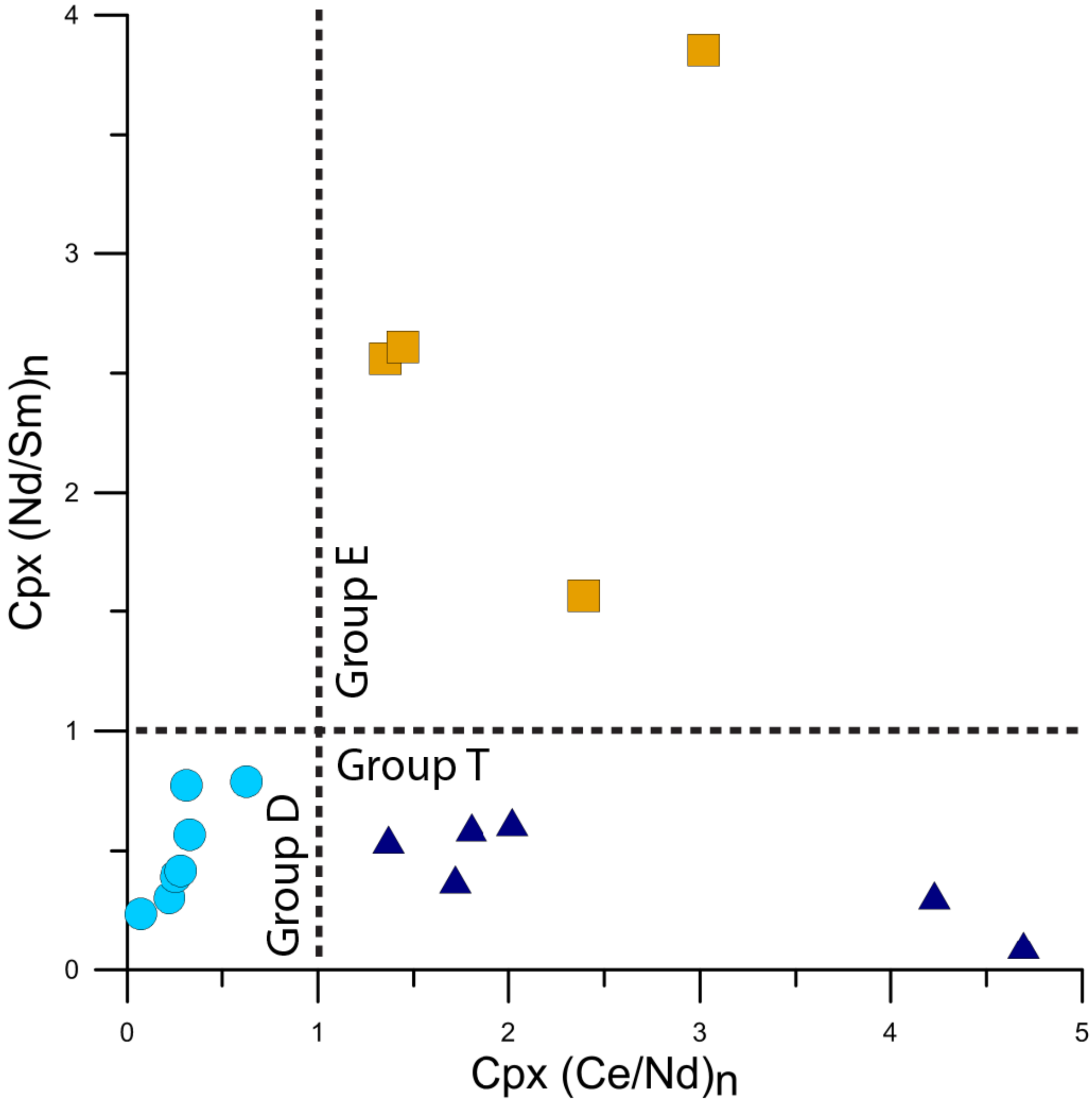

Figure DR1: Groups are defined based on the slope of their REE patterns around Nd. These slopes can be quantified using the ratio of lanthanides with similar incompatibility to Nd. See Figures DR2-4 for individual patterns.

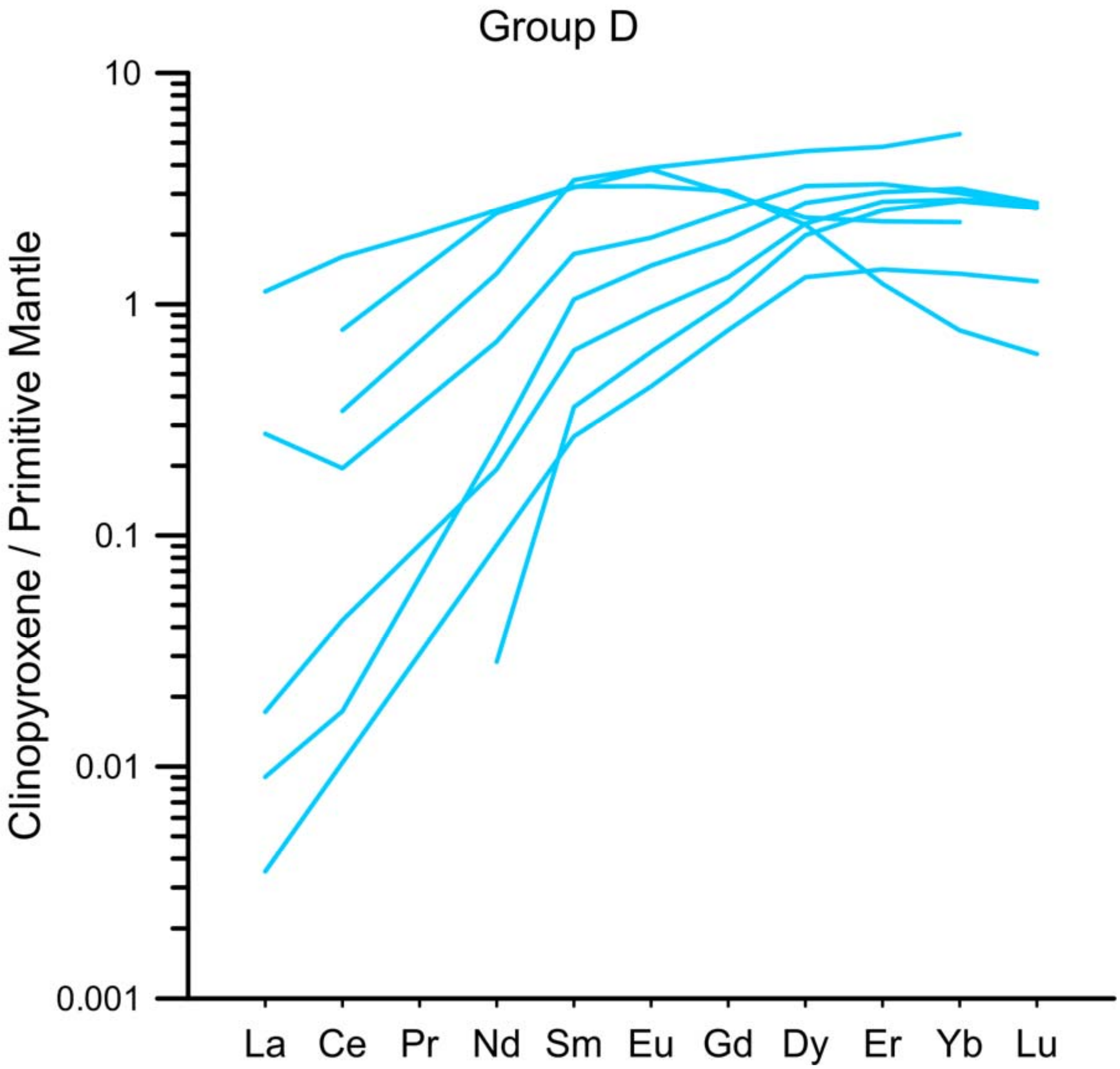

Figure DR2: Rare earth elements in clinopyroxene normalized to primitive mantle (McDonough and Sun, 1995). Group D samples generally display no LREE enrichment, although La is occasionally enriched.

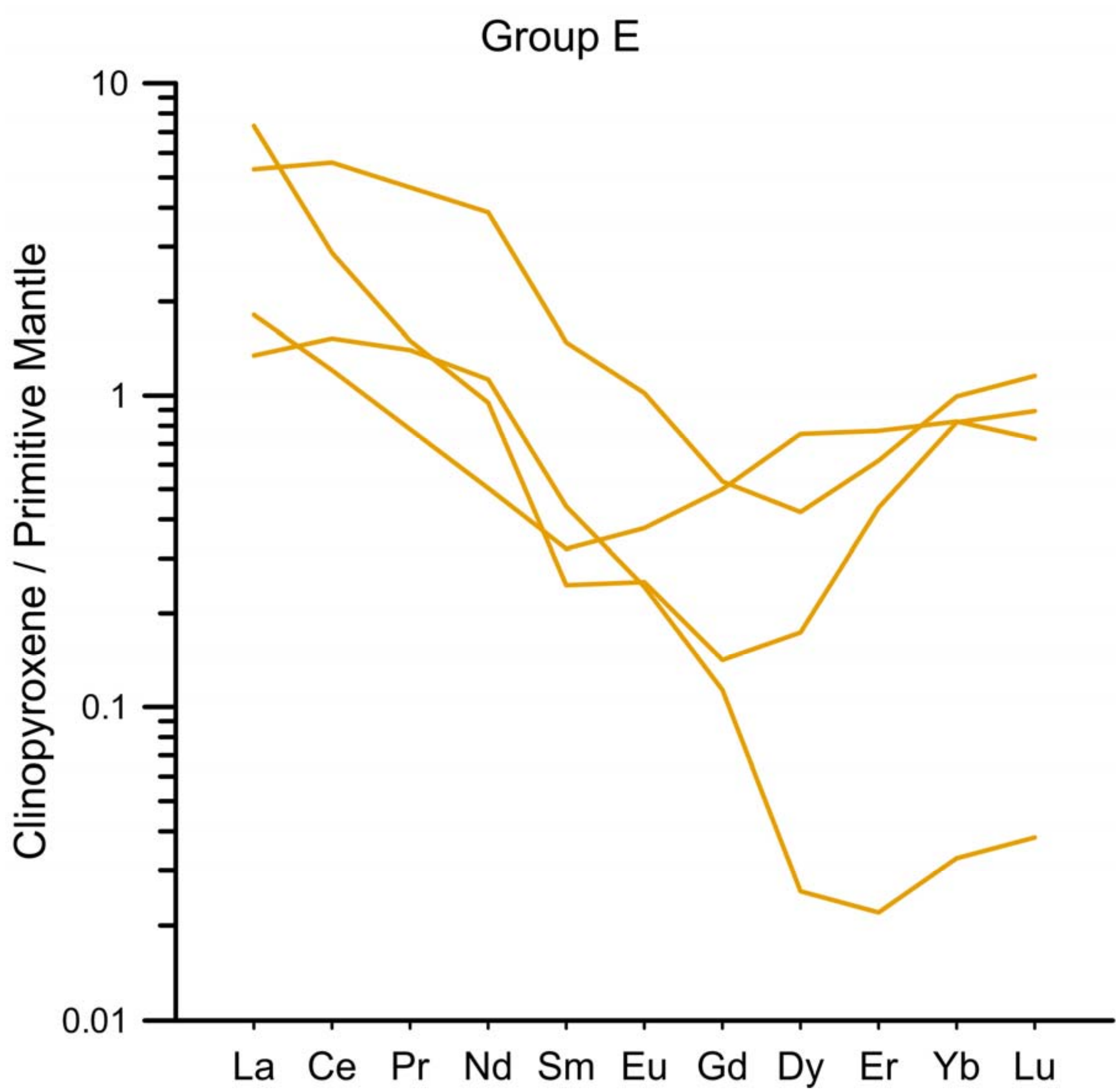

Figure DR3: Rare earth elements in clinopyroxene normalized to primitive mantle (McDonough and Sun, 1995). Group E samples have significant LREE enrichment that certainly affects Nd concentrations.

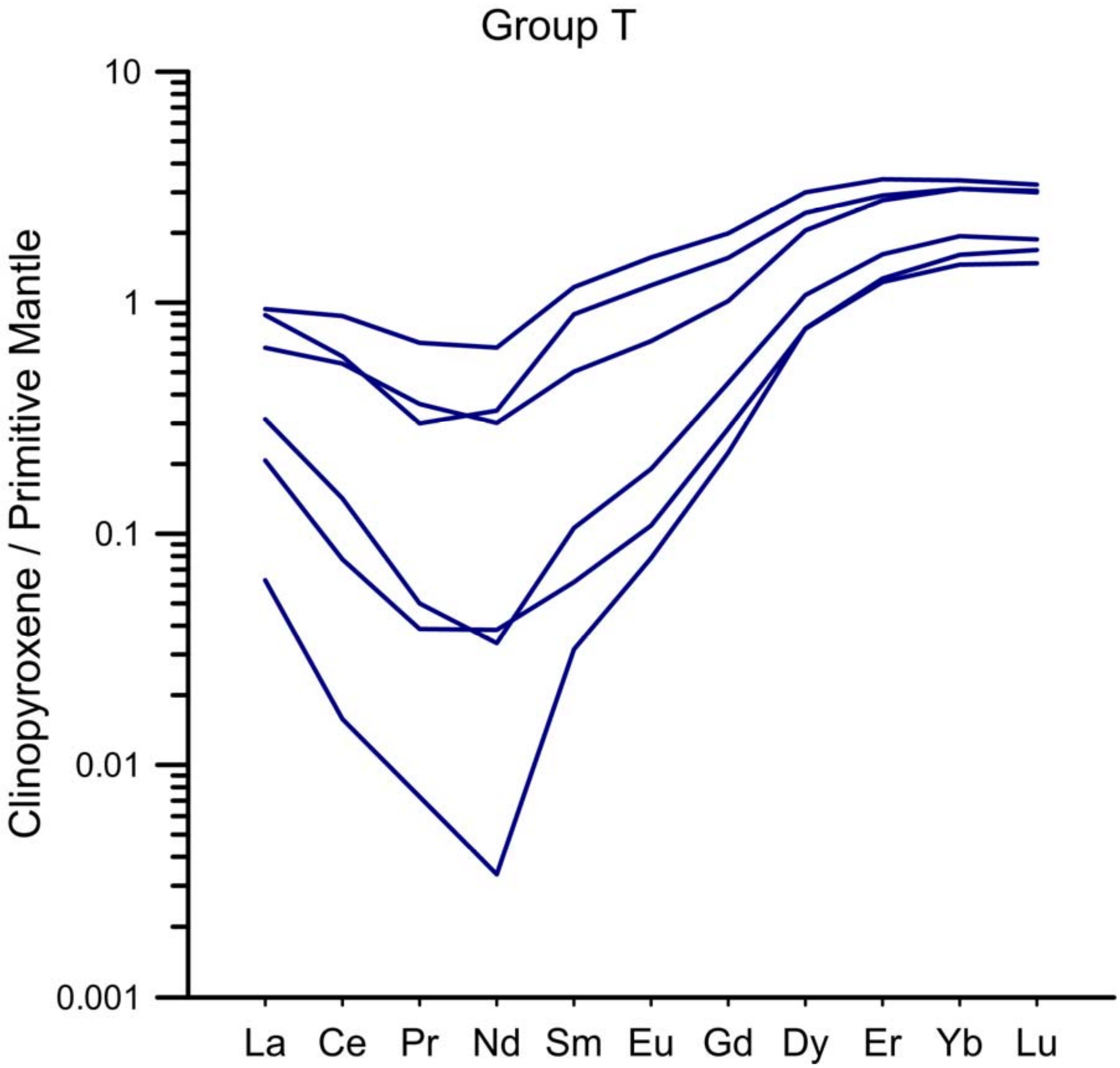

Figure DR4: Rare earth elements in clinopyroxene normalized to primitive mantle (McDonough and Sun, 1995). Group T samples have less LREE enrichment than the Group E samples. However, this LREE enrichment may still affect Nd concentrations.

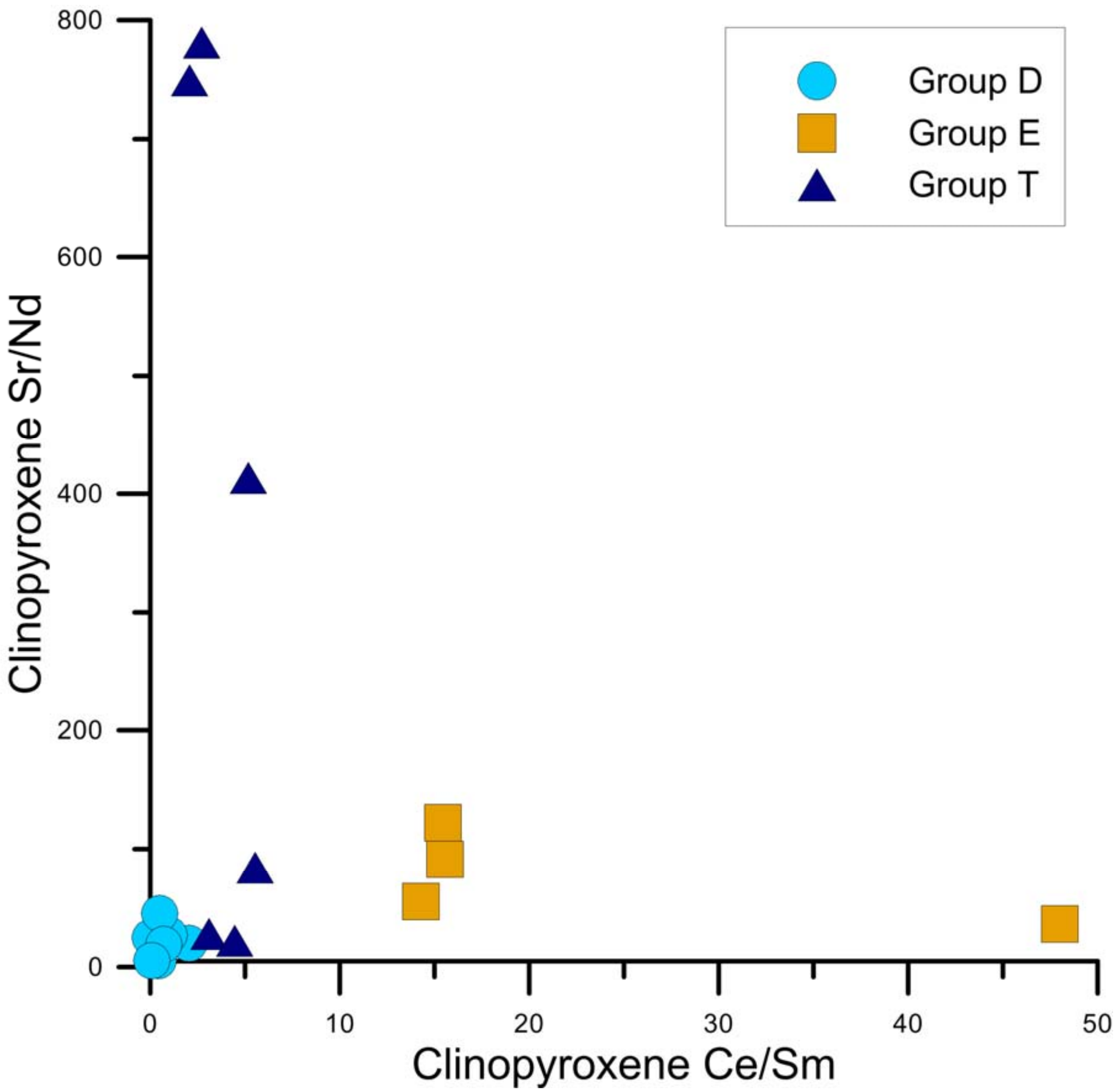

Fig DR5. Ce/Sm in clinopyroxene versus Sr/Nd in clinopyroxene. Group D samples tend to have low Sr/Nd and Ce/Sm. Group E samples tend to be have moderately high Sr/Nd and are LREE enriched. The Group T samples have moderate LREE enrichment and can have extremely high Sr/Nd.

Table DR1: Clinopyroxene major and trace elements

	MR-ATG-13 Average	2σ	N106-GN Average	2σ	N61-GN Average	2σ	EMGN24 Average	2σ	N16-GN Average	2σ	N126-GN Average	2σ	N23-GN Average
	Group D		**Group D**		**Group D R&S (1993)**		**Group D**		**Group D R&S (1993)**		**Group D**		**Group D R&S (1993)**
	n = 5		**n = 8**				**n = 5**				**n = 7**		
SiO2	52.20	(0.06)	52.03	(0.37)	*52.80*		53.25	(0.57)	*51.40*		51.88	(0.12)	*54.10*
TiO2	0.15	(0.02)	0.22	(0.02)	*0.32*		0.48	(0.04)	*0.37*		0.09	(0.01)	*0.33*
Al2O3	5.52	(0.06)	4.84	(0.36)	*5.68*		5.54	(0.63)	*5.95*		6.99	(0.12)	*3.67*
Cr2O3	1.13	(0.04)	0.68	(0.04)	*0.84*		1.04	(0.07)	*0.71*		1.05	(0.04)	*1.35*
FeO	1.98	(0.14)	1.89	(0.11)	*1.76*		2.31	(0.34)	*2.86*		2.21	(0.14)	*1.98*
MnO	0.09	(0.01)	0.06	(0.01)			0.08	(0.01)			0.11	(0.01)	
MgO	15.80	(0.30)	16.60	(0.30)	*14.90*		15.53	(0.75)	*15.10*		15.16	(0.15)	*15.90*
CaO	21.94	(0.37)	22.20	(0.26)	*21.20*		20.18	(0.92)	*22.10*		21.44	(0.19)	*21.00*
Na2O	1.33	(0.04)	1.42	(0.12)	*2.03*		2.04	(0.19)	*1.23*		1.52	(0.09)	*2.28*
Total	100.14		99.96		*99.53*		100.48		*99.72*		100.48		*100.61*
	n = 5		**n = 8**				**n = 5**				**n = 7**		
La	0.01	(0.00)	0.18	(0.05)			0.74	(0.05)			bd		
Ce	0.07	(0.01)	0.33	(0.03)	*1.30*		2.69	(0.13)	*0.58*		bd		*0.93*
Pr							0.51	(0.02)					
Nd	0.24	(0.02)	0.86	(0.11)	*3.10*		3.20	(0.14)	*1.70*		0.04	(0.00)	*2.10*
Sm	0.26	(0.02)	0.67	(0.08)	*1.30*		1.31	(0.05)	*1.40*		0.15	(0.01)	*1.20*
Eu	0.14	(0.01)	0.30	(0.04)	*0.59*		0.50	(0.03)	*0.60*		0.10	(0.00)	*0.41*
Gd	0.71	(0.05)	1.38	(0.14)			1.68	(0.07)			0.56	(0.03)	
Dy	1.50	(0.07)	2.19	(0.28)	*1.60*		1.49	(0.07)	*3.10*		1.33	(0.05)	*0.52*
Er	1.21	(0.07)	1.45	(0.21)	*1.00*		0.54	(0.09)	*2.10*		1.12	(0.04)	*0.26*
Yb	1.25	(0.08)	1.33	(0.23)	*1.00*		0.34	(0.10)	*2.40*		1.23	(0.03)	*0.26*
Lu	0.19	(0.01)	0.18	(0.03)			0.04	(0.01)			0.18	(0.00)	
Rb	0.00	(0.00)	0.01	(0.02)			0.04	(0.02)			0.08	(0.07)	
Th	0.00	(0.00)	0.00	(0.00)			0.01	(0.01)			0.00	(0.00)	
U	0.00	(0.00)	0.01	(0.00)			0.00	(0.00)			0.00	(0.00)	
Nb	0.01	(0.00)	0.01	(0.00)			0.08	(0.02)			0.00	(0.00)	
Ta	0.00	(0.00)	0.00	(0.00)			0.02	(0.00)			0.00	(0.00)	
Pb	0.02	(0.03)	0.30	(0.09)			0.31	(0.19)			0.01	(0.01)	
Sr	5.64	(1.84)	39.40	(7.16)	*85.00*		65.69	(8.62)	*9.50*		0.91	(0.65)	*36.00*
Zr	1.65	(0.08)	5.58	(0.70)	*6.60*		19.37	(0.86)	*7.60*		0.07	(0.01)	*8.70*
Hf	0.11	(0.01)	0.30	(0.01)			0.78	(0.04)			0.02	(0.00)	
Y	9.99	(0.32)	11.75	(1.62)			5.84	(0.64)			9.10	(0.18)	
V	262	(6.58)	229	(10.11)	*260*		316	(14.78)	*280*		240	(5.85)	*420*

Reference: R&S (1993): Roden and Shimizu, (1993); bd: below detection

Table DR1: Clinopyroxene major and trace elements

	N53-GN Average	2σ	EMGN12 Average	2σ	EMMR4 Average	2σ	N55-GN Average	2σ	EMGN21 Average	2σ	N178-GN Average	2σ	EMGN27 Average	2σ
	Group D		Group D		Group D		Group E		Group E		Group E		Group E	
	n = 5		n = 7		n = 1		n = 3		n = 1		n = 7		n = 6	
SiO2	52.25	(1.41)	51.75	(1.21)	53.48		53.53	(0.53)	55.37		54.56	(0.13)	54.91	(3.22)
TiO2	0.20	(0.06)	0.04	(0.07)	0.13		0.05	(0.03)	0.01		0.01	(0.01)	0.00	(0.04)
Al2O3	6.69	(0.89)	5.20	(0.33)	5.36		2.41	(0.84)	1.34		0.72	(0.03)	1.56	(1.01)
Cr2O3	0.90	(0.09)	1.00	(0.16)	1.33		0.50	(0.02)	0.38		0.46	(0.05)	0.98	(1.05)
FeO	2.08	(0.54)	2.04	(0.41)	2.08		1.65	(0.21)	1.26		1.60	(0.07)	1.33	(0.40)
MnO	0.08	(0.05)	0.08	(0.04)	0.13		0.08	(0.02)	0.08		0.06	(0.01)	0.05	(0.06)
MgO	14.84	(1.63)	15.77	(1.91)	15.06		17.53	(0.21)	17.58		17.60	(0.06)	17.47	(0.82)
CaO	21.27	(1.50)	22.42	(2.10)	22.11		23.38	(1.08)	24.10		24.24	(0.07)	23.91	(0.72)
Na2O	1.90	(0.24)	1.00	(0.27)	1.47		0.69	(0.26)	0.57		0.58	(0.06)	0.79	(0.25)
Total	100.29	(1.73)	99.36	(1.07)	101.17		99.87		100.72		99.86		101.01	
	n = 6		n = 8		n = 2		n = 3		n = 1		n = 7		n = 9	
La	0.01	(0.00)	0.01	(0.01)	bd		1.17	(0.22)	4.75		3.44	(0.28)	0.87	(0.27)
Ce	0.03	(0.00)	0.01	(0.01)	bd		2.02	(0.27)	4.80		9.36	(0.30)	2.55	(0.77)
Pr	0.02	(0.00)	0.00		bd				0.38				0.36	(0.11)
Nd	0.31	(0.02)	bd		bd		0.63	(0.06)	1.19		4.84	(0.51)	1.41	(0.46)
Sm	0.43	(0.05)	0.02	(0.00)	0.11	(0.02)	0.13	(0.03)	0.10		0.60	(0.09)	0.18	(0.06)
Eu	0.23	(0.02)	0.02	(0.01)	0.07	(0.01)	0.06	(0.01)	0.04		0.16	(0.02)	0.04	(0.01)
Gd	1.03	(0.08)	0.15	(0.04)	0.42	(0.04)	0.27	(0.07)	0.08		0.29	(0.04)	0.06	(0.03)
Dy	1.85	(0.13)	0.57	(0.06)	0.88	(0.10)	0.51	(0.19)	0.12		0.28	(0.02)	0.02	(0.01)
Er	1.34	(0.08)	0.57	(0.08)	0.62	(0.06)	0.34	(0.17)	0.19		0.27	(0.02)	0.01	(0.01)
Yb	1.40	(0.13)	0.70	(0.06)	0.60	(0.12)	0.36	(0.17)	0.36		0.44	(0.02)	0.01	(0.01)
Lu	0.19	(0.02)	0.11	(0.02)	0.08	(0.01)	0.05	(0.02)	0.06		0.08	(0.00)	0.00	(0.00)
Rb	bd		bd		bd		0.13	(0.12)	0.37		0.04	(0.02)	0.38	(0.74)
Th	0.00	(0.00)	bd		bd		0.04	(0.01)	0.28		0.00	(0.00)	0.02	(0.03)
U	bd		bd		0.03	(0.09)	0.04	(0.01)	0.05		0.01	(0.00)	0.01	(0.01)
Nb	0.01	(0.00)	0.00	(0.00)	bd		0.49	(0.28)	0.20		0.00	(0.00)	0.02	(0.04)
Ta							0.00	(0.00)	0.02		bd			
Pb							0.54	(0.22)	0.97		1.12	(0.22)		
Sr	1.81	(0.33)	0.59	(0.94)	4.05	(9.79)	77.27	(22.65)	43.49		443.00	(87.52)	78.57	(93.60)
Zr	1.00	(0.10)	bd		0.28	(0.05)	0.05	(0.01)	0.28		1.39	(0.13)	0.28	(0.08)
Hf	0.12	(0.02)	0.00	(0.00)	0.05	(0.01)	0.02	(0.01)	0.01		0.06	(0.01)	0.01	(0.01)
Y	11.30	(0.81)	4.39	(0.45)	5.44	(0.42)	2.94	(1.35)	1.20		1.97	(0.08)	0.08	(0.05)
V							199	(41.49)	171		141	(4.77)		

Reference: R&S (1993): Roden and Shimizu, (1993); bd: below detection

Table DR1: Clinopyroxene major and trace elements

	EMMR25 Average	2σ	EMGN6 Average	2σ	EMGN29 Average	2σ	EMGN9 Average	2σ	EMGN2 Average	2σ	N17-GN Average	2σ	NMNH Cr-Augite Average	2σ
	Group T		Group T		Group T		Group T		Group T		Group T			
	n = 1		n = 1		n = 6		n = 4		n = 4		n = 10		n = 36	
SiO2	56.06		53.25		51.75	(1.02)	53.61	(1.58)	52.87	(0.45)	51.85		50.66	(1.19)
TiO2	0.02		0.05		0.04	(0.01)	0.11	(0.05)	0.20	(0.01)	0.04		0.48	(0.08)
Al2O3	0.37		4.92		5.44	(0.83)	4.20	(1.30)	5.62	(0.47)	5.07		8.06	(0.28)
Cr2O3	0.06		1.06		1.11	(0.23)	0.79	(0.32)	0.76	(0.03)	1.06		0.87	(0.12)
FeO	1.99		2.52		2.03	(0.35)	1.65	(0.19)	2.23	(0.35)	1.88		4.80	(0.32)
MnO	0.12		0.09		0.08	(0.02)	0.09	(0.01)	0.09	(0.02)	0.08		0.13	(0.03)
MgO	18.12		16.12		15.77	(1.04)	15.86	(0.64)	15.64	(0.89)	15.91		17.25	(0.40)
CaO	24.23		21.93		22.33	(0.99)	22.68	(0.55)	21.14	(1.52)	23.08		17.28	(0.31)
Na2O	0.46		0.88		1.24	(0.23)	1.40	(0.24)	1.52	(0.11)	1.01		0.83	(0.16)
Total	101.54		100.91		99.85		100.41	(0.73)	100.07		100.00		100.38	
	n = 2		n = 2		n = 6		n = 5		n = 4		n = 10			
La	0.57	(0.07)	0.20	(0.01)	0.03	(0.09)	0.40	(0.09)	0.61	(0.03)	0.04	(0.01)		
Ce	0.98	(0.14)	0.24	(0.01)	0.02	(0.07)	0.89	(0.16)	1.46	(0.05)	0.03	(0.01)		
Pr	0.08	(0.02)	0.01	(0.00)	0.00	(0.00)	0.09	(0.02)	0.17	(0.00)				
Nd	0.43	(0.20)	0.04		bd		0.37	(0.07)	0.79	(0.03)	bd			
Sm	0.36	(0.17)	0.04		0.02	(0.01)	0.20	(0.04)	0.47	(0.03)	0.01	(0.00)		
Eu	0.18	(0.05)	0.03	(0.00)	0.02	(0.02)	0.10	(0.02)	0.24	(0.01)	0.01	(0.00)		
Gd	0.85	(0.21)	0.24	(0.03)	0.18	(0.03)	0.55	(0.10)	1.08	(0.05)	0.12	(0.01)		
Dy	1.65	(0.48)	0.73	(0.05)	0.61	(0.05)	1.37	(0.18)	2.00	(0.10)	0.52	(0.02)		
Er	1.28	(0.35)	0.71	(0.05)	0.59	(0.05)	1.21	(0.14)	1.49	(0.03)	0.56	(0.03)		
Yb	1.37	(0.30)	0.85	(0.01)	0.70	(0.04)	1.36	(0.15)	1.47	(0.08)	0.71	(0.04)		
Lu	0.20	(0.03)	0.13	(0.00)	0.11	(0.01)	0.21	(0.03)	0.22	(0.01)	0.11	(0.01)		
Rb	bd		0.58	(0.68)	0.23	(0.24)	0.11	(0.10)	0.02	(0.01)	bd			
Th	bd		0.01		bd		0.01	(0.01)	0.03	(0.00)	bd			
U	0.21	(0.08)	0.00	(0.00)	0.01	(0.01)	0.01	(0.01)	0.01	(0.00)	0.01	(0.00)		
Nb	bd		0.57	(0.00)	0.00	(0.00)	0.22	(0.19)	0.30	(0.05)	0.004	(0.001)		
Ta					0.00	(0.00)	0.01	(0.00)	0.02	(0.00)	bd			
Pb					0.09	(0.33)	0.11	(0.18)	0.04	(0.03)	0.03	(0.01)		
Sr	332.85	(79.62)	3.55	(0.09)	3.47	(10.68)	8.05	(6.21)	22.71	(0.69)	3.15	(1.27)		
Zr	0.32	(0.03)	0.01		0.00	(0.01)	1.29	(0.19)	0.81	(0.03)	bd			
Hf	0.04	(0.01)	0.00	(0.00)	bd		0.04	(0.01)	0.11	(0.01)	bd			
Y	10.36	(2.73)	5.59	(0.45)	4.57	(0.42)	9.36	(1.11)	12.42	(0.45)	4.22	(0.18)		
V					217	(13.46)	246	(21.82)	238	(1.61)	233	(5.20)		

Reference: R&S (1993): Roden and Shimizu, (1993); bd: below detection

Table DR1: Clinopyroxene major and trace elements

	BCR-2G Average	2σ	N17-GN*	N23-GN*
			Group T	Group D
			Smith and Levy (1976)	*Smith (1979)*
SiO2			*52.30*	*54.70*
TiO2			*0.08*	*0.08*
Al2O3			*4.44*	*1.73*
Cr2O3			*0.85*	*1.24*
FeO			*2.16*	*2.03*
MnO			*0.10*	*0.06*
MgO			*17.30*	*16.80*
CaO			*21.90*	*22.60*
Na2O			*0.91*	*1.19*
Total			*100.04*	*100.43*
	n = 22			
La	25.50	(1.33)		
Ce	54.50	(3.14)		
Pr	6.46	(0.11)		
Nd	29.14	(1.27)		
Sm	6.75	(0.31)		
Eu	1.97	(0.10)		
Gd	6.55	(0.36)		
Dy	6.40	(0.29)		
Er	3.61	(0.15)		
Yb	3.42	(0.18)		
Lu	0.51	(0.03)		
Rb	47.90	(1.98)		
Th	5.97	(0.22)		
U	1.70	(0.09)		
Nb	12.60	(0.72)		
Ta	0.78	(0.03)		
Pb	10.60	(0.49)		
Sr	349.28	(14.48)		
Zr	178.11	(7.66)		
Hf	4.61	(0.17)		
Y	32.91	(1.58)		
V	442	(12.83)		

Reference: R&S (1993): Roden and Shimizu, (1993); bd: below detection

***: These previously published analyses are included for easy comparison with the analyses used in this publication**

Table DR2: Whole Rock major and trace elements

Sample	MR-ATG-13	N61-GN§*	EMGN24	N16-GN§*	N126-GN	N23-GN*	EMGN12	EMMR4	N106-GN	N55-GN	EMGN21	N178-GN§	
	Group D	Group D	Group D	Group D	Group D	Group D	Group D	Group D	Group D	Group E	Group E	Group E	
												n = 3	**2σ**
SiO_2	43.82	44.68	43.45	40.62	45.00	42.64	43.25	44.04	45.21	43.19	43.37	43.22	(0.92)
TiO_2	0.02	0.09	0.10	0.03	0.02	0.07	0.01	0.02	0.06	0.01	0.00	0.00	(0.00)
Al_2O_3	1.98	2.71	2.54	2.12	2.54	4.45	1.72	2.00	3.67	1.91	0.96	0.81	(0.33)
Cr_2O_3	0.47	0.37	0.35	0.35	0.37	0.28	0.35	0.47	0.47	0.34	0.23	0.30	(0.14)
FeO	7.65	8.12	7.24	10.15	7.79	7.37	7.18	6.71	7.71	8.18	7.15	7.04	(0.22)
MnO	0.12	0.12	0.11	0.14	0.12	0.11	0.12	0.05	0.13	0.12	0.13	0.11	(0.00)
MgO	40.27	39.88	35.59	42.99	39.11	36.69	40.21	32.52	37.80	42.37	42.33	44.89	(1.93)
CaO	1.60	2.42	3.15	1.50	2.40	2.46	1.71	1.66	3.25	2.35	1.11	0.55	(0.35)
Na_2O	0.05	0.24	0.30	0.07	0.14	0.46	0.15	0.28	0.36	0.21	0.02	0.02	(0.00)
K_2O	0.01	0.00	0.04	0.01	0.00	0.07	0.01	0.09	0.01	0.02	0.01	0.00	(0.00)
NiO	0.29	0.26	0.20	0.36	0.27	0.19	0.29	0.28	0.25	0.31	0.24	0.32	(0.03)
P_2O_5	0.00	0.01	0.00	0.01	0.01	0.05	0.00	0.00	0.01	0.00	0.00	0.00	(0.00)
LOI	3.77	0.90	6.08	1.64	2.42	5.12	4.77	11.40	1.15	1.21	4.38	2.97	(0.24)
Total	100.05	99.81	99.15	100.00	100.18	99.96	99.76	99.52	100.07	100.25	99.92	100.24	
La	0.03	0.18	0.19	0.11	0.05	0.71	0.05	0.08	0.11	0.38	0.19	0.14	(0.06)
Ce	0.06	0.58	0.44	0.22	0.11	0.84	0.10	0.13	0.16	0.56	0.32	0.35	(0.16)
Pr	0.01	0.12	0.07	0.06	0.01	0.10	0.01	0.01	0.02	0.06	0.04	0.04	(0.02)
Nd	0.04	0.63	0.36	0.18	0.04	0.42	0.04	0.04	0.15	0.16	0.16	0.17	(0.09)
Sm	0.01	0.24	0.17	0.09	0.03	0.19	0.01	0.02	0.13	0.03	0.04	0.03	(0.01)
Eu	0.01	0.10	0.07	0.04	0.01	0.08	0.00	0.01	0.06	0.01	0.01	0.01	(0.01)
Gd	0.03	0.27	0.26	0.15	0.07	0.31	0.02	0.04	0.23	0.06	0.03	0.02	(0.01)
Tb	0.01	0.05	0.05	0.03	0.02	0.07	0.01	0.01	0.05	0.02	0.00	0.00	(0.00)
Dy	0.08	0.31	0.33	0.23	0.19	0.48	0.07	0.07	0.40	0.14	0.03	0.01	(0.01)
Ho	0.02	0.07	0.07	0.06	0.05	0.11	0.02	0.02	0.09	0.04	0.01	0.00	(0.00)
Er	0.07	0.17	0.19	0.17	0.15	0.33	0.07	0.06	0.29	0.12	0.03	0.02	(0.01)
Tm	0.01	0.03	0.03	0.02	0.03	0.05	0.01	0.01	0.04	0.02	0.01	0.00	(0.00)
Yb	0.11	0.17	0.19	0.16	0.18	0.30	0.09	0.06	0.30	0.14	0.04	0.02	(0.01)
Lu	0.02	0.03	0.03	0.03	0.03	0.05	0.01	0.01	0.05	0.02	0.01	0.00	(0.00)
Rb	0.09	0.34	0.10	0.65	0.11	0.30	0.17	0.73	0.11	0.30	0.14	0.23	(0.04)
Pb	0.07	0.39	0.10	0.25	0.11	1.62	0.43	1.90	0.65	1.54	0.32	0.19	(0.06)
Th	0.01	0.02	0.01	0.04	0.01	0.05	0.02	0.00	0.01	0.03	0.06	0.02	(0.01)
U	0.20	0.01	0.01	0.01	0.00	0.03	0.00	3.99	0.01	0.03	0.01	0.01	(0.00)
Nb	0.02	0.05	0.04	0.06	0.03	0.29	0.02	0.03	0.02	0.72	0.14	0.03	(0.01)
Sr	34.14	19.97	22.93	7.96	11.60	117.00	13.82	50.93	16.60	26.75	11.91	14.71	(6.41)
Zr	0.34	1.56	0.27	1.20	0.39	1.73	0.36	0.13	1.18	0.36	0.30	0.33	(0.21)
Hf	0.01	0.03	0.01	0.05	0.01	0.07	0.01	0.01	0.05	0.01	0.01	0.01	(0.00)
Y	0.56	1.63	0.19	1.44	1.23	2.79	0.52	0.49	2.37	0.97	0.22	0.10	(0.05)
Sc	11.69	11.77	7.94	7.63	11.97	14.33	9.95	10.17	13.95	10.90	7.30	7.42	(2.36)
V	56.46	63.28	73.44	37.68	57.98	75.92	47.91	64.72	73.32	48.43	33.99	25.81	(9.15)

§: Previously published whole rock analyses are available in Smith (1979), Smith (2010). *: Previously published whole rock trace element analyses available in Roden et al., (1990).

Table DR2: Whole Rock major and trace elements

Sample	EMGN27	N17-GN§*	EMGN2	EMMR25	EMGN6	EMGN29	EMGN9	EMGN37	BHVO-2	
	Group E	Group T	Group T	Group T	Group T	Group T	Group T	N/A		
										published
SiO2	42.02	45.61	44.76	44.95	44.53	46.04	43.58	40.52	49.88	49.90
TiO2	0.00	0.01	0.04	0.05	0.02	0.01	0.02	0.00	2.76	2.73
Al2O3	0.98	2.00	2.73	3.60	2.42	2.51	2.20	0.41	13.61	13.50
Cr2O3	0.27	0.42	0.24	0.52	0.38	0.45	0.41	0.44	0.04	0.04
FeO	6.74	7.27	7.60	7.60	6.77	7.14	7.28	7.18	11.18	11.07
MnO	0.11	0.12	0.12	0.07	0.11	0.12	0.12	0.12	0.17	0.17
MgO	41.53	40.93	39.01	29.85	36.76	37.76	38.77	44.44	7.30	7.23
CaO	0.57	1.86	2.60	2.95	2.67	2.20	2.07	0.33	11.42	11.40
Na2O	0.03	0.13	0.27	0.24	0.35	0.10	0.25	0.00	2.23	2.22
K2O	0.02	0.01	0.02	0.10	0.04	0.01	0.05	0.00	0.52	0.52
NiO	0.23	0.27	0.21	0.29	0.24	0.24	0.26	0.31	0.01	0.02
P2O5	0.00	0.00	0.00	0.00	0.00	0.00	0.00	0.00	0.26	0.27
LOI	6.78	1.67	1.31	8.76	5.47	2.90	4.52	5.82	0.00	0.00
Total	99.29	100.31	98.92	98.98	99.76	99.47	99.52	99.59	99.37	99.06
La	0.06	0.16	0.19	0.19	0.18	0.09	0.16	0.11	15.29	15.20
Ce	0.07	0.23	0.30	0.36	0.37	0.11	0.29	0.14	36.95	37.50
Pr	0.01	0.03	0.04	0.04	0.04	0.01	0.04	0.01	5.26	5.29
Nd	0.03	0.08	0.15	0.19	0.17	0.02	0.15	0.03	24.14	24.50
Sm	0.00	0.02	0.05	0.10	0.03	0.00	0.03	0.01	6.41	6.07
Eu	0.00	0.00	0.03	0.04	0.01	0.00	0.02	0.00	2.19	2.07
Gd	0.00	0.02	0.15	0.17	0.06	0.02	0.07	0.01	6.42	6.24
Tb	0.00	0.01	0.04	0.04	0.01	0.01	0.01	0.00	1.02	0.94
Dy	0.00	0.06	0.27	0.31	0.11	0.08	0.15	0.01	5.68	5.31
Ho	0.00	0.02	0.07	0.08	0.03	0.02	0.04	0.00	1.05	0.97
Er	0.00	0.07	0.20	0.24	0.11	0.08	0.12	0.01	2.61	2.54
Tm	0.00	0.01	0.03	0.04	0.02	0.01	0.02	0.00	0.35	0.34
Yb	0.01	0.09	0.22	0.24	0.14	0.11	0.14	0.01	1.94	2.00
Lu	0.00	0.01	0.04	0.04	0.02	0.02	0.02	0.00	0.28	0.27
Rb	0.49	0.22	0.34	1.03	0.35	0.23	0.46	0.40	8.94	9.08
Pb	0.23	0.59	0.46	0.94	0.61	0.20	0.62	0.40	1.60	1.40
Th	0.02	0.03	0.03	0.03	0.02	0.01	0.02	0.01	1.24	1.18
U	0.01	0.01	0.02	3.70	0.02	0.03	0.03	0.01	0.42	0.44
Nb	0.00	0.06	0.06	0.09	0.12	0.01	0.07	0.06	16.80	16.40
Sr	7.74	19.84	28.17	118.99	19.56	17.36	20.88	10.52	394.86	396.00
Zr	0.39	0.53	0.57	0.71	0.74	0.31	0.51	0.28	166.20	160.00
Hf	0.01	0.01	0.03	0.03	0.02	0.00	0.01	0.01	4.42	4.10
Y	0.31	0.48	1.76	2.07	0.89	0.59	0.92	0.06	25.60	23.00
Sc	9.74	11.33	12.61	14.80	13.32	12.69	11.57	4.85	31.86	31.00
V	28.12	57.29	60.74	89.63	58.94	66.48	54.46	21.67	312.47	317.00

§: Previously published whole rock analyses are available in Smith (1979), Smith (2010). *: Previously published whole rock trace element analyses available in Roden et al., (1990).

Table DR3: Whole rock Osmium isotope compositions.

		187Re/188Os	187Os/188Os	Os	Re	Whole Rock Al_2O_3	Rhenium Depletion age (Ga)
EMMR04	**Group D**	1.82	0.12053(4)	4.99	1.92	2.00	1.2
EMGN24	**Group D**	0.49	0.1260(3)	3.89	0.40	2.54	0.5
N23-GN	**Group D**	0.37	0.1272(2)	3.31	0.26	4.45	0.3
EMGN12	**Group D**	0.19	0.12428(5)	4.46	0.17	1.72	0.7
N178-GN	**Group E**	0.27	0.1188(10)	2.97	0.17	0.81	1.5
N178-GN*	**Group E**	0.08	0.11521(6)	2.70	0.04	0.81	2.0
EMGN27	**Group E**	0.22	0.1171(5)	2.88	0.13	0.98	1.7
EMGN27*	**Group E**	nd	0.11596(7)	4.65	nd	0.98	1.9
EMMR25*	**Group T**	0.24	0.1287(2)	2.98	0.15	3.60	0.1
EMGN6	**Group T**	0.65	0.12704(3)	3.57	0.49	2.42	0.4
EMGN6*	**Group T**	0.33	0.12672(5)	5.20	0.37	2.42	0.4
EMGN2	**Group T**	0.27	0.12556(2)	3.62	0.21	2.73	0.6
EMGN9	**Group T**	*nd*	0.12611(3)	3.44	*nd*	2.20	0.5
EMGN9*	**Group T**	0.15	0.1256(5)	3.14	0.10	2.20	0.5
EMGN29	**Group T**	*nd*	0.12663(3)	3.27	*nd*	2.51	0.4
EMGN37	**N/A- no cpx**	9.84	0.1140(1)	0.76	1.59	0.41	2.1

*: Sample digested at University of Bonn; *nd*: not determined

Table DR4: Sm-Nd isotope analyses

		First Round (soft leach)				Second Round (hard leach)			
		Sm (ppm)	**Nd (ppm)**	**147Sm/144Nd**	**143Nd/144Nd**	**Sm (ppm)**	**Nd (ppm)**	**147Sm/144Nd**	**143Nd/144Nd**
MR-ATG-13	**Group D**	0.215(1)	0.199(1)	0.6541(35)	0.517359(44)				
EMGN24	**Group D**	0.933(3)	2.232(9)	0.2530(14)	0.513432(2)				
N16-GN[1]	**Group D**	*0.886*	*1.28*	*0.4180(42)*	*0.514800(60)*				
N61-GN[1]	**Group D**	*1.42*	*3.89*	*0.2210(22)*	*0.513102(25)*				
N106-GN	**Group D**					0.550(4)	0.719(6)	0.4624(49)	0.515414(5)
N126-GN	**Group D**	0.1050(3)	0.0270(1)	2.3569(126)	0.533395(14)	0.189(1)	0.0469(3)	2.4298(259)	0.533356(28)
N53-GN	**Group D**					0.401(3)	0.292(2)	0.8300(88)	0.518925(13)
EMGN21	**Group E**	0.313(1)	1.468(6)	0.1288(7)	0.512474(4)				
N55-GN	**Group E**	0.184(1)	0.975(4)	0.1143(6)	0.512586(8)				
N178-GN	**Group E**	0.497(2)	3.729(15)	0.0805(4)	0.512889(7)				
EMGN2	**Group T**	0.383(1)	0.669(3)	0.3462(19)	0.514290(3)	0.252(2)	0.654(5)	0.2335(25)	0.514291(28)
N17-GN	**Group T**	0.0230(1)	0.154(1)	0.0921(5)	0.513172(5)	0.0193(1)	0.106(1)	0.1103(12)	0.513320(10)

[1]: Roden, Smith and Murthy, (1990)

All concentrations determined via isotope dilution, errors are 2σ